International Journal of Nanomedicine

Dovepress
open access to scientific and medical research

Open Access Full Text Article

ORIGINAL RESEARCH

Long-Circulation and Brain Targeted Isoliquiritigenin Micelle Nanoparticles: Formation, Characterization, Tissue Distribution, Pharmacokinetics and Effects for Ischemic Stroke

Weitong Song[1], Lu Bai[1], Yuya Yang[1], Yongchao Wang[2], Pingxiang Xu[1,3], Yuming Zhao[1], Xuelin Zhou[1,3], Xiaorong Li[1,3], Ming Xue[1,3]

[1]Department of Pharmacology, School of Basic Medical Sciences, Capital Medical University, Beijing, People's Republic of China; [2]CAS Key Laboratory for Biomedical Effects of Nanomaterials and Nanosafety, CAS Center for Excellence in Nanoscience, National Center for Nanoscience and Technology of China, Beijing, People's Republic of China; [3]Beijing Laboratory for Biomedical Detection Technology and Instrument, Beijing, People's Republic of China

Correspondence: Ming Xue, Department of Pharmacology, School of Basic Medical Sciences, Capital Medical University, Youanmen, Beijing, 100069, People's Republic of China, Tel +8610-83950416, Fax +8610-83911520, Email xuem@ccmu.edu.cn

Purpose: We designed a novel isoliquiritigenin (ISL) loaded micelle prepared with DSPE-PEG_{2000} as the drug carrier modified with the brain-targeting polypeptide angiopep-2 to improve the poor water solubility and low bioavailability of ISL for the treatment of acute ischemic stroke.

Methods: Thin film evaporation was used to synthesize the ISL micelles (ISL-M) modified with angiopep-2 as the brain targeted ligands. The morphology of the micelles was observed by the TEM. The particle size and zeta potential were measured via the nanometer particle size analyzer. The drug loading, encapsulation and in vitro release rates of micelles were detected by the HPLC. The UPLC-ESI-MS/MS methods were used to measure the ISL concentrations of ISL in plasma and main tissues after intravenous administration, and compared the pharmacokinetics and tissue distributions between ISL and ISL-M. In the MCAO mice model, the protective effects of ISL and ISL-M were confirmed via the behavioral and molecular biology experiments.

Results: The results showed that the drug loading of ISL-M was 7.63 ± 2.62%, the encapsulation efficiency was 68.17 ± 6.23%, the particle size was 40.87 ± 4.82 nm, and the zeta potential was −34.23 ± 3.35 mV. The in vitro release experiments showed that ISL-M had good sustained-release effect and pH sensitivity. Compared with ISL monomers, the ISL-M could significantly prolong the in vivo circulation time of ISL and enhance the accumulation in the brain tissues. The ISL-M could ameliorate the brain injury induced by the MCAO mice via inhibition of cellular autophagy and neuronal apoptosis. There were no the cellular structural damages and other adverse effects for ISL-M on the main tissues and organs.

Conclusion: The ISL-M could serve as a promising and ideal drug candidate for the clinical application of ISL in the treatment of acute ischemic stroke.

Keywords: isoliquiritigenin, micelle, brain distribution, pharmacokinetics, ischemic stroke, MCAO

Introduction

Cerebral stroke was defined as the formation of thrombus or blood clots on basis of the pathological changes in the brain arteries, while the blood flow was slow, the blood composition changed or the blood viscosity increased, which caused the lesion and blockage in the blood vessels.[1] Approximately 87% of strokes have been accounted for the ischemic strokes, and it was the second most common cause of mortality and permanent disability worldwide.[2] Up to now, intravenous thrombolysis and thrombectomy are the major therapeutic strategies and methods, and this procedure is often accompanied by cerebral ischemia-reperfusion injury, which results in aggravating brain damage with very few effective

Received: 29 March 2022
Accepted: 28 July 2022
Published: 17 August 2022

treatments. Thus, it is very important and urgent to develop the novel drugs or new methods to prevent and treat ischemic stroke in early phase.[3]

Isoliquiritigenin (ISL) is one of the major active flavonoid glycosides extracted from *Glycyrrhiza uralensis*, which has shown the markedly pharmacological activities, such as anti-inflammatory, anti-oxidant and anti-tumor.[4–6] The results also showed that ISL had a good protective effect on cerebral ischemia-reperfusion injury.[7] However, the pharmacokinetic studies had found that there were the poor oral absorption, low bioavailability and brain tissue distribution, and short half-life for ISL compound in vivo. These weakness of in vivo disposition for ISL largely limited the effective application of the drug in clinical practice.

In order to effectively increase the exposure and circulation levels of ISL in the targeted tissue, the polymeric micelle system was successfully designed and used to improve the physicochemical and structural properties of drug such as solubility resulting in that the circulation time was prolonged and the immunogenicity was reduced.[8–11] DSPE-PEG_{2000} is an amphiphilic polymer which could be formed into the core-shell structured nanoparticles by self-assembly methods. In this study, we designed and prepared the ISL loaded micelles made of 1,2-distearoyl-sn-glycero-3-phosphoethanolamine-N-[methoxy (polyethylene glycol)-2000] (DSPE-PEG_{2000}), which was proved safe, biocompatible and relatively non-toxic, and had been approved by the Food and Drug Administration of United States of American (FDA, USA).[12,13] The hydrophobic groups formed by the long fatty acyl chains could load the fat soluble drug molecules, which efficiently restricted the mobility of drugs at the same time, leading to a sustained drug release. Furthermore, a polyethylene glycol (PEG) surface-modified nanoparticles could enhance the circulation time in blood, reduce the clearance rate by the reticuloendothelial system (RES), and prolong the circulation time of the drug-loaded micelles.[14,15]

The existence of blood–brain barrier (BBB) could effectively prevent some drugs from penetrating into the brain. To overcome this barrier, it was an effective method to modify the nano micelles with the specific brain targeted ligands binding to the endogenous receptors on the BBB, resulting in drugs across the BBB more easily.[16–18] Angiopep-2 (Ang) was a novel polypeptide composed of nineteen amino acids, it could enter the brain tissue via the low-density lipoprotein receptor-related protein 1 (LRP-1) receptor mediated endocytosis, which expressed on the BBB.[19] In addition, the nano drug modified with angiopep-2 could significantly improve the accumulation of drugs in the brains. Compared with lactoferrin (LF) and transferrin (TF) which were the major brain targeted modification ligands with endogenous competition,[20] the BBB penetration efficiency of angiopep-2 was several times higher than that in LF and TF.[21]

Based on these considerations, the DSPE-PEG_{2000} modified with the brain-targeting peptide angiopep-2 was used as the effective carrier to prepare the ISL micelles (ISL-M) for treatment of brain injury induced by acute ischemic stroke. In this study, the ISL nano micelles were designed and prepared to improve pharmacokinetic characteristics, increase the accumulation level of ISL in the brain, ameliorate the neuronal damage and reverse the behavioral deficits cause by ischemic stroke. In addition, there was no any obvious toxicity in main tissues and organs after intravenous administration of ISL-M. The data from our present experiments showed that the ISL-M was a novel, effective and safe drug candidate for the treatment of ischemic stroke.

Materials and Methods

Materials

Isoliquiritigenin (MW=256.25, Purity>95%) [(e)-1-(2,4-dihydroxyphenyl)-3-(4-hydroxyphenyl) −2-propen-1-one] was purchased from the Tokyo Chemical Industry Co., Ltd (Tokyo, Japan). DSPE-mPEG_{2000} [1, 2-distearoyl-sn-glycero-3-phosphoethanolamine-N-methoxy (polyethylene glycol)-2000] was provided by the Lipoid GmbH (Ludwigshafen, Frigenstrasse, German). DSPE-PEG_{2000}-Mal [1, 2-distearoyl-sn-glycero-3-phosphoethanolamine-N-MaleiMide (polyethylene glycol)-2000] was obtained from the Shanghai Ponsure Biotechnology Co., Ltd (Shanghai, China). Angiopep-2 (CTFFYGGSRGKRNNFKTEEY) was synthesized by the Shanghai Top Biological Technology Co., Ltd (Shanghai, China). Tris (2-carboxyethyl) phosphine (TCEP) was obtained by the Beijing Solarbio Science and Technology Co., Ltd (Beijing, China). MCAO monofilaments were purchased from Beijing Cinotech Co., Ltd (Beijing, China). Hematoxylin-eosin staining was provided by the Wuhan Service Bio-technology Co., Ltd (Wuhan, Hubei, China). TUNEL staining was obtained from the Beyotime Biotechnology (Nantong, Jiangsu, China). Antibodies

were purchased from Cell Signaling Technology (Beverly, Massachusetts, USA). Acetonitrile was supported as HPLC grade by the Fisher Scientific (Fair Lawn, NJ, USA). All other chemicals and solvent were of analytical grade.

Synthesis of DSPE-PEG2000-Angiopep-2

Maleimide-functionalized copolymer DSPE-PEG_{2000}-Angiopep-2 was synthesized by linking DSPE-PEG_{2000}-Mal to angiopep-2 through a carbodiimide-mediated coupling reaction. 6 mg of DSPE-PEG_{2000}-Mal, 5 mg of angiopep-2 and 5 mg of TCEP were weighed accurately and dissolved with 50 mM HEPES buffer (pH = 7) in pear shaped bottle. After ultrasonic mixing for 20 min, the mixture was stirred magnetically under the protection of nitrogen for 4 h at room temperature. Then the solution was dialyzed in a dialysis bag (MWCO = 3500) for 24 h, freeze-dried and stored for use in a refrigerator at −20 °C.

Preparation of ISL-M

ISL micelle was prepared by the methods of thin-film rotary evaporation. First, the ISL was fully dissolved in methanol, DSPE-PEG_{2000} was dissolved in dichloromethane, DSPE-PEG_{2000}-Angiopep-2 dissolved in chloroform, respectively, and then these compounds were mixed. Subsequently, the organic solvent was removed via vacuum rotary evaporation at a temperature of 45 °C, the rotating speed was 130 rpm for 20 min. After hydration with normal saline, the suspension was sonicated for 20 min and filtered by a nylon filter (0.22 μm) to obtain the ISL micelles.

Characterization of ISL-M

UV-Visible Spectroscopy

DSPE-PEG_{2000}-Mal, DSPE-PEG_{2000}-Angiopep-2 and angiopep-2 were dissolved in deionized water, respectively, and detected by the UV-2600 spectrophotometer (Shimadzu, Kyoto, Japan).

Fourier Transform Infrared Spectrometer (FT-IR)

The chemical structures of DSPE-PEG_{2000}-Mal, DSPE-PEG_{2000}-Angiopep-2 and angiopep-2 were measured by attenuated total reflection (ATR) with a Nicolet iS5 Fourier transform infrared spectrometer (Thermo Fisher Scientific, MA, USA).

^{1}H-NMR Spectrometer

5 mg of DSPE-PEG_{2000}-Mal, DSPE-PEG_{2000}-Angiopep-2 and angiopep-2 were dissolved in 1 mL of DMSO-d6, respectively, and analyzed in the 400 MHz NMR spectrometer (Bruker Daltonics Lnc., Blairika, Massachusetts, USA).

Particle Size, Polydispersity Index, and Zeta Potential

The freshly made micelles were diluted appropriately with distilled water. The particle size, particle dispersion index (PDI) and zeta potential (ZP) of ISL micelles were measured by the Zeta-sizer Nano S90 (Malvern Instruments, U.K.).

Morphology of ISL-M

The micromorphology of the ISL micelles was observed by 120 kV HT7700 transmission electron microscope (Hitachi, Tokyo, Japan).

Encapsulation Efficiency and Drug Loading Capacity of ISL-M

The concentrations of ISL were detected by the high-performance liquid chromatography (HPLC) system (Agilent Technologies, Santa Clara, USA), the sample separation was performed on the ZORBAX SB-C_{18} column (5 μm, 4.6 × 150 mm, Agilent) with a flow rate of 1.0 mL/min. The isocratic mobile phase was consisted of 0.1% formic acid aqueous solution and acetonitrile (50:50, v/v), and the detection wavelength of ISL was set at 367 nm.

The ISL micelles were dissolved in methanol and sonicated for 20 min. After centrifuging at 13,000 rpm for 10 min, the supernatant was filtered through a nylon filter (0.22 μm) and 20 μL was injected into HPLC. The encapsulation efficiency (EE) of ISL micelles was calculated as the following formula:

$$EE\ (\%) = \text{Weight of loaded drug} / \text{Weight of drug in feeding} \times 100\%$$

The drug loading capacity (DLC) of ISL micelles was calculated as the following formula:

$$DLC\ (\%) = \text{Weight of loaded drug} / \text{Weight of micelles} \times 100\%$$

In vitro Release Studies

As described similarly in the previous study,[22] the ISL-loaded micelles were transferred into a pre-soaked dialysis bag (MWCO = 500), immersed in 50 mL of release medium (PBS buffer with 1% SDS), and shaken with speed of 200 rpm at 37 °C. 0.2 mL of the outside PBS was withdrawn for measurements at predetermined time intervals (0.5, 1, 2, 4, 6, 8, 12, 24 and 48 h) and an equal volume of the fresh PBS was supplemented. The accumulative release amounts of ISL were analyzed and calculated using the HPLC system as described above.

LC-MS/MS Determination for ISL and ISL-M in vivo

The UPLC-MS/MS system consisted of Agilent 1290 series with LC pump and auto-sampler (Agilent, Santa Clara, USA), coupled with an Agilent 6490 triple quadrupole mass spectrometer (Agilent Technologies, Santa Clara, USA) equipped with the electrospray ionization (ESI). Chromatographic separation was implemented by the Eclipse Plus C_{18} column (100 × 2.1 mm i.d., 1.8 μm, Agilent Technologies, USA) under isocratic mobile phase compositions using 0.1% formic acid aqueous solution and acetonitrile (60:40, v/v) with a flow rate of 0.3 mL/min.

The column temperature was set at 25 °C and the autosampler temperature was 4 °C. The MS/MS system was operated under the negative mode with an optimized condition as follows: ion spray voltage at +5.5 kV, nitrogen as nebulizer gas, auxiliary gas and curtain gas was at 30, 60 and 10 psi, respectively. The auxiliary gas temperature was at 225 °C and interface heater temperature at 110°C. The multiple reaction monitoring (MRM) analyses were conducted by monitoring the precursor ion to production transitions, including the m/z 255 → 119 for ISL and the m/z 268 → 133 for genistein (the internal standard, IS). 100 μL of plasma sample was spiked with 300 μL of acetonitrile and 100 μL of IS (1 μg/mL). After vortexing, the mixture was centrifuged 13,000 rpm for 10 min at 4 °C. The supernatant (400 μL) was collected followed by being evaporated to dryness under nitrogen at room temperature. The residue was reconstituted with 200 μL of methanol, filtered through a nylon filter (0.22 μm) and 5 μL aliquot was injected into the UPLC-MS/MS system for analyses.

The LC-ESI-MS/MS method for quantification of ISL in plasma and tissue was validated for accuracy, precision, selectivity, linearity, recovery and matrix effect according to the guidelines of US FDA bioanalytical method.

Pharmacokinetics and Tissue Distribution of ISL-M and ISL

Sprague Dawley (SD) male rats (aging 7-9 weeks, 240-260 g) were purchased from the Beijing Animal Science Biotechnology Co., Ltd (Beijing, China). All animal procedures were performed in accordance with the guidelines for Care and Use of Laboratory Animals for Capital Medical University and approved by the Animal Ethics Committee of Capital Medical University.

The rats were randomly divided into two groups, with six rats in each group and fasted overnight before the experiment. ISL (dissolved in physiological saline containing 30% propylene glycol) and ISL micelles were injected via the tail vein at a dose of 2 mg/kg, respectively. The blood samples (100 μL) were obtained from the jugular vein and collected in the heparin pretreated polypropylene centrifuge tubes at each time point (0.03, 0.08, 0.17, 0.33, 0.5, 1, 2, 4 and 8 h) over a period of 8 h after the administration. The plasma was isolated by centrifuging at 13,000 rpm for 10 min at 4 °C and then stored at −80 °C for further analysis. The pharmacokinetic analysis was processed with the program DAS 2.0 Pharmacokinetics Software (Chinese Pharmacological Society, Beijing, China).

ICR male mice (aging 6-8 weeks, 27-28 g) were purchased from Beijing Vital River Laboratory Animal Technology Co., Ltd (Beijing, China). The mice were randomly divided into two groups and these two formulations of ISL at a dose of 2.8 mg/kg were administered via intravenous route. At each predetermined time point (0.17, 0.5, 1 and 2 h) after dosing, four mice for each test point were sacrificed for collection of heart, liver, lung, kidney, and brain, respectively. The tissues were rinsed with normal saline, weighed and homogenized with cold saline (w/v=1:2). Subsequently, the

tissue homogenates were centrifuged at 13,000 rpm for 10 min. The supernatant was transferred into the tube, and stored at −80 °C until analysis.

The maximum concentration (C_{max}) in tissues was obtained from the observed data, and the values of area under the curve (AUC) for the drug concentration with time were calculated by the linear trapezoidal method.[23] The relative rate of uptake (R_e) of each tissue was the ratio of AUC for ISL-M to AUC for ISL in this tissue, and the ratio of peak concentration (C_p) of each tissue was the ratio of C_{max} of ISL-M to C_{max} of ISL in the tissue.

The Middle Cerebral Artery Ischemia (MCAO) Model

C57BL/6 mice (male, aging 6-8 weeks, 24-26 g) were purchased from the Beijing Vital River Laboratory Animal Technology Co., Ltd (Beijing, China), which were randomly divided into six groups, with four mice each group. The groups were the group for the sham, MCAO model, 3 mg/kg dose of ISL, 1 mg/kg dose of ISL micelles, 3 mg/kg dose of ISL micelles, and 3 mg/kg dose of edaravone (EDA). The MCAO model in mice was used for experiments as previously described.[24]

The mice were anesthetized with 5% chloral hydrate by intraperitoneal injection before the experiment. The suitable incision in neck was conducted to fully expose the field of view for operation, and the right common carotid artery (CCA), external carotid artery (ECA) and internal carotid artery (ICA) from the peripheral connective tissues were separated. The surgical monofilament (1620-A4, Beijing Cinotech Co., Ltd) was slowly inserted into ICA via the ECA stump until the resistance occurred, indicating that it had blocked the starting point of the middle cerebral artery (MCA). Then the surgical monofilament was fixed, the wound was covered with cotton moistened with normal saline and the mice were housed in an incubator at 37 °C. One hour later, the monofilament was removed to restore blood flow. Sham-operated mice underwent the same procedures without insertion of the monofilament. After the operation, the mice in different groups were intravenously injected for 7 days with corresponding drugs. Then the mice were sacrificed and perfused with PBS (pH = 7) and 4% paraformaldehyde. The brain tissue was collected to slice into frozen sections with a thickness of 20 μm and stored at −80 °C refrigerator.

The Effects of Drug on the MCAO Model Mice

Longa Scores

The neurological examination was used to assess the neurological deficits of MCAO mice.[24] The test was conducted by the investigator who was blinded to treat the tested groups. The neurologic findings were scored on a 5-point scale as follows: a score of 0, with no neurologic deficit; a score of 1, failure to extend left forepaw fully; a score of 2, walking in a circle to the left; a score of 3, falling to the left; and a score of 4, unable to walk spontaneously and a depression in consciousness.

Adhesive Removal Test

The sensorimotor function in animals was evaluated by using adhesive removal test after stroke, as described in the previous studies.[25] Patches of adhesive tape (3 mm × 4 mm) were attached to the right front paws of mice with equal pressure by the experimenter before each trial. The mice were placed in a test box, and the times to contact and to remove adhesive tape were recorded with a maximum of 120 s, respectively. The mice were trained for three days, and tested for three times on the seventh day after operation conducted.

Rotarod Experiments

The rotarod experiment was used to evaluate the neurological function of mice.[26] The mice were trained on the rotarod (DXP-2, Institute of Materia Medica, Chinese Academy of Medical Sciences) for three days after surgery. The speed on the first day was 6 rpm, the speed on the second day and the third day was 14 rpm. The latency to fall was recorded as the time before mice fell off the rotarod with the beginning speed for 14 rpm.

Hematoxylin-Eosin Staining of Tissue for Toxicity Study

The C57BL/6 mice in each group were intravenously injected with ISL and different doses of ISL-M, respectively, the unloaded micelles or the ISL micelles for the in vivo toxicity study. The organs in mice including the heart, liver, spleen,

lung and kidney, were all collected and fixed in 4% paraformaldehyde. The frozen tissue sections were used for hematoxylin and eosin (H&E) staining, and the tissue toxicity was observed by a brightfield microscope.

Nissl Staining of Tissue for Neuronal Injury

The frozen sections of brains in mice were immersed in the Nissl staining solution (Sigma) at room temperature for 20 min. The slides were then sealed with neutral balsam after dehydration with different concentrations of ethanol, and washing with xylene for 5 min. Observations of neuronal injury were performed using a brightfield microscope.

TUNEL Staining for Apoptosis of Nerve Cell

The TUNEL assay was employed to observe the apoptosis of nerve cells in the MCAO model. According to the instructions of the TUNEL kit (Beyotime Biotechnology), the frozen sections of brain tissues for each group in mice were fluorescently stained to observe the broken nuclear DNA fragments. The number of cells with significant fluorescence in different fields of view were recorded by the image J software.

Immunofluorescence Staining for Autophagy of Nerve Cell

The frozen slides were baked in a 37 °C oven for 10–20 min and fixed in paraformaldehyde for 30 min. After washing three times with PBS (pH = 7.4) for 5 min, the sections were immersed in EDTA antigen retrieval buffer (pH = 8.0), and maintained at a sub-boiling temperature for 8 min, standing for 8 min, and then followed by another sub-boiling temperature for 7 min. Wash three times with PBS (pH = 7.4), 5 min each time, and add 3% BSA to cover the marked tissue to block non-specific binding for 30 min. The immunostaining was performed by incubating with primary antibody rabbit Anti-LC3 (1:100, Cell Signaling Technology) overnight at 4 °C followed by secondary antibody Cy3 conjugated goat anti-rabbit IgG H&L (1:300, Wuhan Servicebio Technology Co., Ltd) at room temperature for 50 min. The brain sections were rinsed three times in PBS (pH = 7.4) for 5 min each, and then incubated with DAPI solution (Wuhan Servicebio Technology Co., Ltd) at room temperature for 10 min in order to observe the cell nuclei by a laser confocal fluorescence microscope. The images from the junction of infarction and intact areas were randomly captured and processed for counting the number of cells with significant fluorescence by the image J.

Statistical Analysis

The data of the experiments were summarized as the mean ± standard deviation (SD). The image processing and image analyses were performed using the Image J software, version 1.43 for Windows. The statistical analysis was performed by one-way ANOVA or unpaired *t*-test and followed by SPSS 19.0 statistical software. The differences were considered statistically significant at $P < 0.05$.

Results and Discussion

Design and Preparation of ISL-M

Scheme 1 showed the design and synthetic routes of DSPE-PEG_{2000}-Angiopep-2 under the protection condition of nitrogen and the reduction of TCEP. The DSPE-PEG_{2000}-Angiopep-2, DSPE-PEG_{2000} and ISL were mixed in a distillation flask to prepare the ISL nano micelles by thin film evaporation. The prepared micelles were successfully injected into the MCAO mice by intravenous administration, uptaken across the blood-brain barrier via the blood circulation. The transport mechanism of the micelles was investigated and recognized, indicating that the LRP-1 receptor mediated endocytosis into the blood-brain barrier.[19]

Characterization of DSPE-PEG_{2000}-Angiopep-2

The spectra of UV, FT-IR and ^{1}H-NMR were used to characterize the compounds of DSPE-PEG_{2000}-Angiopep-2 by linking DSPE-PEG_{2000}-Mal to the thiol moiety of angiopep-2. Compared with the UV absorption nature of DSPE-PEG_{2000}-Mal, the UV absorption of DSPE-PEG_{2000}-Angiopep-2 was significantly shifted to the blue wave side, and coincided with the UV characteristic absorption of angiopep-2 near 270 nm (Figure 1A). As shown in Figure 1B, there was obvious enhancement of the peak near 3300 cm^{-1} in the infrared spectra of DSPE-PEG_{2000}-Angiopep-2 due to the hydroxyl group existed in angiopep-2. The peaks existed at 1650–1690 cm^{-1} and 1500–1600 cm^{-1} were ascribed to

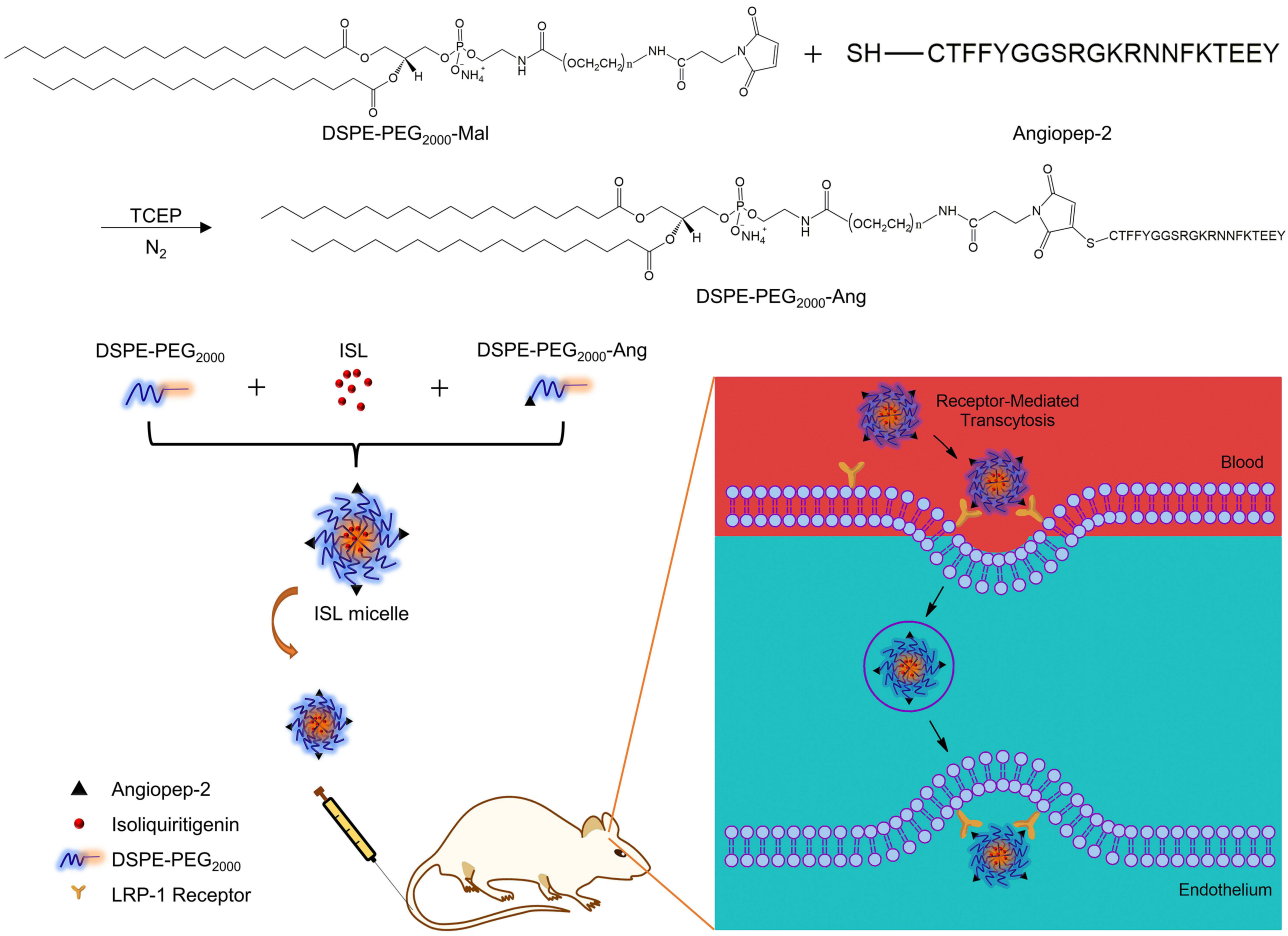

Scheme 1 Preparation of ISL micelles and its mechanism of LRP-1 receptor-mediated penetration of the blood-brain barrier.
Abbreviations: LRP-1, low-density lipoprotein receptor-related protein 1; ISL, isoliquiritigenin; ISL-M, isoliquiritigenin micelles.

stretching vibration of the amide bond and benzene ring. Figure 1C1 showed the ^{1}H-NMR spectrum of Angiopep-2 had a large number of H peaks from benzene ring and amide bond in chemical shifts 6.5 to 8.5 ppm. Compared with DSPE-PEG$_{2000}$-Mal that had a characteristic peak of maleimide group at the chemical shift of 6.5 ppm, shown in Figure 1C2, the Mal peak disappeared in the ^{1}H-NMR spectra of DSPE-PEG$_{2000}$-Angiopep-2 and was replaced by lots of H peaks around chemical shifts 6.5 to 8.0 ppm (see the Figure 1C3). The results of three kinds of spectra confirmed that the Mal group had reacted with the thiol moiety of angiopep-2.

Characterization of ISL-M

DSPE-PEG$_{2000}$, as an amphiphilic molecule, could self-assemble to form the polymer micelles composed of a hydrophobic core formed by DSPE and a hydrophilic shell formed by PEG$_{2000}$ in aqueous solution via filming-rehydration method.[27]

Our results that the encapsulation efficiency and drug loading of ISL-M were 68.17 ± 6.23% and 7.63 ± 2.62%, respectively. The average particle size of ISL-M was 40.87 ± 4.82 nm with a good distribution (PDI, 0.26 ± 0.01) (see the Figure 2A). Previous studies had shown that the nanoparticles with a particle size of less than 10 nm were easy to be quickly removed by the kidney,[28,29] and nanoparticles with a particle size of greater than 200 nm would be rapidly eliminated by activating the complement system from the blood stream.[30–32] Further, most in vitro studies had shown that the uptake of nanoparticles by cells was mainly in the particle size range of 10~60 nm.[33–37] Based on these studies, it would be inferred that ISL-M could prolong the circulation time in vivo and be better uptaken by cells.[28–37]

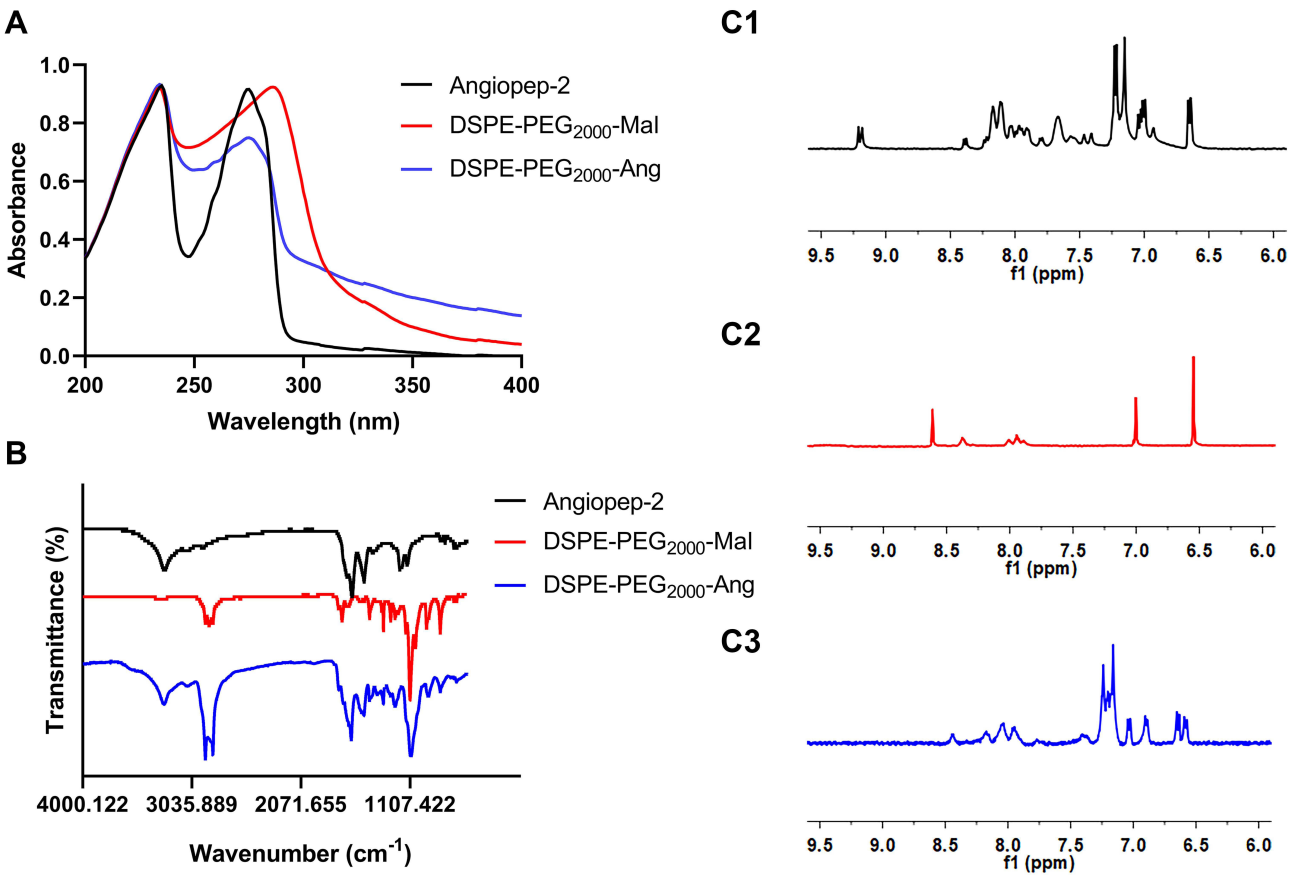

Figure 1 Characterization of the DSPE-PEG_{2000}-Ang. The UV (**A**) and FT-IR spectra (**B**) of angiopep-2, DSPE-PEG_{2000}-Mal and DSPE-PEG_{2000}-Ang; ^{1}H-NMR spectra of angiopep-2 (**C1**), DSPE-PEG_{2000}-Mal (**C2**) and DSPE-PEG_{2000}-Ang (**C3**).
Abbreviations: UV, ultraviolet; FT-IR, fourier transform infrared spectroscopy; ^{1}H NMR, nuclear magnetic resonance H spectrum.

The observation via the TEM (Figure 2B) showed that the micelles were spherical and well-dispersed in the aqueous solution, which could be uptaken by cells more easily than non-spherical nanoparticles.[38] Generally, the absolute value of zeta potential above 30 mV could be considered as relatively stable for the dispersion system and it was difficult to agglomerate. The higher the absolute value of zeta potential, the greater the repulsive force among the charges on surface of nanoparticles, and the better the dispersion of nanoparticles.[39] In our study, the zeta potential of ISL-M was −34.23 ± 3.35 mV (shown in Figure 2C), indicating that ISL-M had good dispersion.

The in vitro release profiles of the free ISL and ISL-M were investigated at simulated in vivo conditions using phosphate-buffered saline (pH = 7.4 and pH = 5, 37 °C) containing 1% (w/v) sodium dodecyl sulfate (Figure 2D). More than 60% of free ISL in PBS buffer (pH = 7.4 and pH = 5) was rapidly released within the first four hours, and the cumulative release was close to 90% in eight hours. Whereas, the cumulative release rate of ISL-M slowed down significantly at pH of 5 and reached more than 90% after 48 h dialysis. Under the condition of pH of 7.4, the release rate of ISL-M was the slowest, and only about 60% of ISL was released within 48 hours. These results suggested that of this nano-micelle had good slow-release effect and pH sensitivity, which prevented drugs from being released as fast as possible during blood circulation (pH = 7.4) so that it could maintain a sustained higher drug concentration in an environment of cerebral ischemia and hypoxia. In addition, the nano micelles uptaken by nerve cells could quickly release drugs in lysosomes (pH = 4.5~5.0) and take effects as follow. In general, excellent physicochemical properties and biological effects would help nano micelles play a better role in drug delivery.[40]

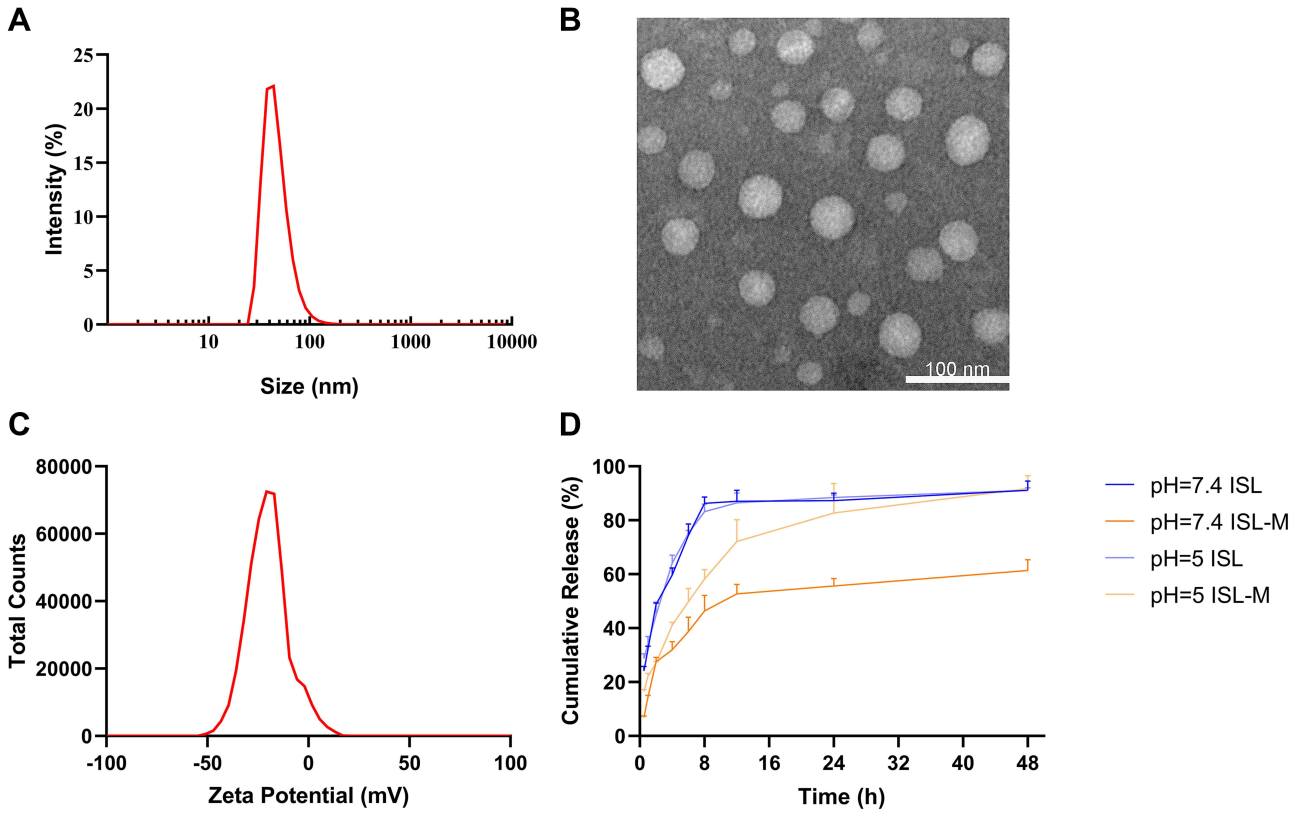

Figure 2 The physicochemical properties of ISL-M. (**A**) Particle size distribution of ISL-M; (**B**) TEM image of ISL-M; (**C**) zeta potential of ISL-M; (**D**) in vitro release profile of ISL and ISL-M in PBS at pH = 7.4 and 5.

Note: Data was presented as the mean ± SD, n = 3.

Abbreviations: TEM, transmission electron microscope; PBS, phosphate buffer saline.

Validation of Analytical Method

In order to determine the concentration of ISL in plasma and tissue, the LC-MS/MS methods were established for this study. The retention times of IS and ISL in plasma were 2.4 min and 3 min, respectively, while those in tissues were 1.7 min and 2.1 min, respectively (Supporting Information Figure S1A and S1B). There were no endogenous substances interfered in plasma and tissue matrix (Supporting Information Figure S1C and S1D), indicating that there was good specificity of these methods. After intravenous injection of ISL-M, there was no significant shift in the retention time of ISL and IS in rat plasma and mixed tissue homogenate (Supporting Information Figure S1E and S1F), indicating that the method has good stability.

The regression equation of standard curve in plasma for the low concentration range (5–2000 ng/mL) was $y = 0.004391x + 0.004727$ ($R^2 = 0.9998$) and for the high concentration range (2–100 μg/mL) was $y = 3.867x + 0.7097$ ($R^2 = 0.9999$). In addition, the calibration curve for the tissues was also identified within the range of 5–1000 ng/mL

($y = 0.001869x - 0.007118$, $R^2 = 0.9990$). Therefore, the linearity of these methods was excellent. The lower limit of quantification (LLOQ) in plasma and in tissue was 5 ng/mL, shown in Supporting Information Table S1.

The intra-day and inter-day precision (RSD %) of quality control (QC) samples in both matrices were all less than 13.78%, while the accuracy (RE %) ranged from −6.57% to 7.32% for ISL in two matrices (Supporting Information Table S2). The recovery of ISL was between 88.08% to 104.73%, and the results of the matrix effect were in the range of 86.31-107.82% for all the QC samples (Supporting Information Table S3). These data indicated that the precision, accuracy and extraction recovery of QC samples with three different concentrations were within an acceptable range according to the FDA guidelines, and no significantly matrix effect was found for the plasma and tissue homogenate.

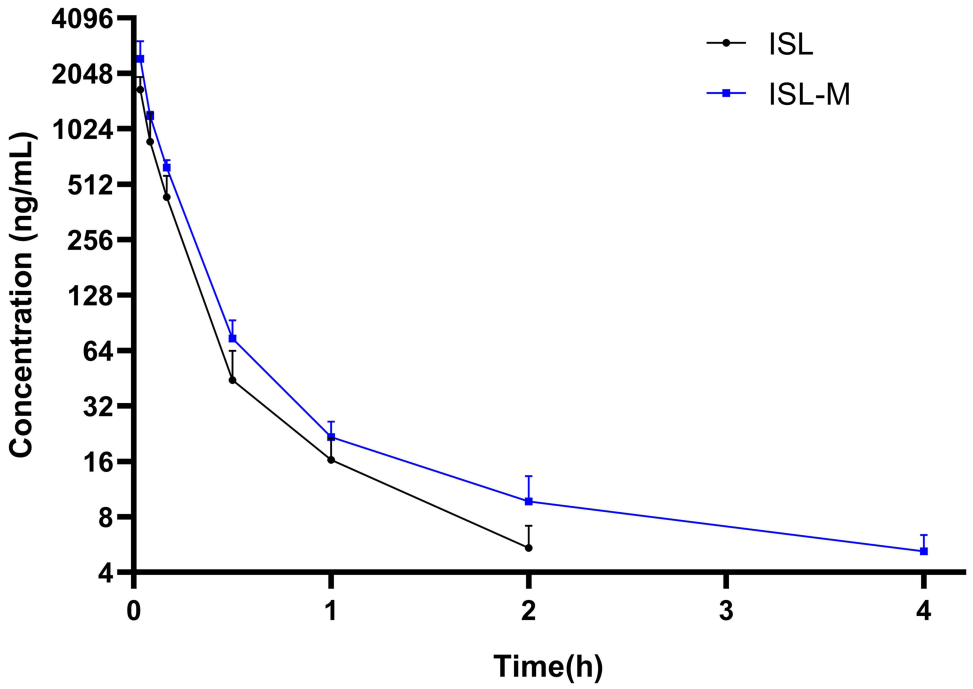

Figure 3 The mean plasma concentration-time curve of ISL and ISL-M after a single intravenous injection (2 mg/kg) to rats.
Note: Data was presented as the mean ± SD, n = 6.

Pharmacokinetics Profiles of ISL and ISL-M

The plasma concentration-time profile of ISL and ISL-M after single intravenous administration of 2 mg/kg in rats was shown in Figure 3. The concentration of ISL in plasma for the ISL group was low, and could not be detected after 2 hours of administration, while the ISL-M group could be detected within 4 hours. The data in Table 1 summarized the pharmacokinetic parameters of ISL and ISL-M, which were calculated according to the compartment model and statistical moment theory. The results showed that the plasma elimination half-life ($t_{1/2\beta}$) of ISL-M was markedly prolonged by 2.6 times compared with that of ISL. The AUC of ISL-M was significantly higher than that of ISL, suggesting that the in vivo exposure of ISL from ISL-M notably increased, and the mean residence time (MRT) of ISL-M had also been obviously prolonged. The clearance rate of ISL and ISL-M was 5.78 L/h.kg and 3.64 L/h.kg, respectively, indicating that the elimination speed of ISL-M was slower than that of ISL in rat. ISL-M has high relative bioavailability of 148.96%. Our results indicating that ISL-M could effectively prolonged the circulation time of ISL, markedly increased the in vivo exposure amount and significantly improved the pharmacokinetic properties of ISL.

Table 1 Pharmacokinetic Parameters of ISL After Single I.V. Administration of ISL and ISL-M (2 Mg/Kg) to Rats

Parameters	Unit	ISL	ISL-M
$t_{1/2\alpha}$	h	0.07 ± 0.01	0.09 ± 0.01
$t_{1/2\beta}$	h	0.70 ± 0.22	1.82 ± 0.35*
AUC (0-t)	ng/mL*h	306.78 ± 92.53	459.05 ± 40.32*
AUC (0-∞)	ng/mL*h	372.75 ± 105.57	555.25 ± 60.42*
MRT (0-t)	h	0.17 ± 0.03	0.26 ± 0.03***
CL	L/h/kg	5.78 ± 1.74	3.64 ± 0.39*
F_{rel}	%		148.96

Notes: The results were expressed as the mean ± SD, n = 6; vs ISL group: *$P < 0.05$, ***$P < 0.001$.
Abbreviations: $t_{1/2\alpha}$, distribution half-life; $t_{1/2\beta}$, elimination half-life; AUC, area under the plasma concentration–time curve; MRT, mean residence time; CL, clearance rate; F_{rel}, relative bioavailability.

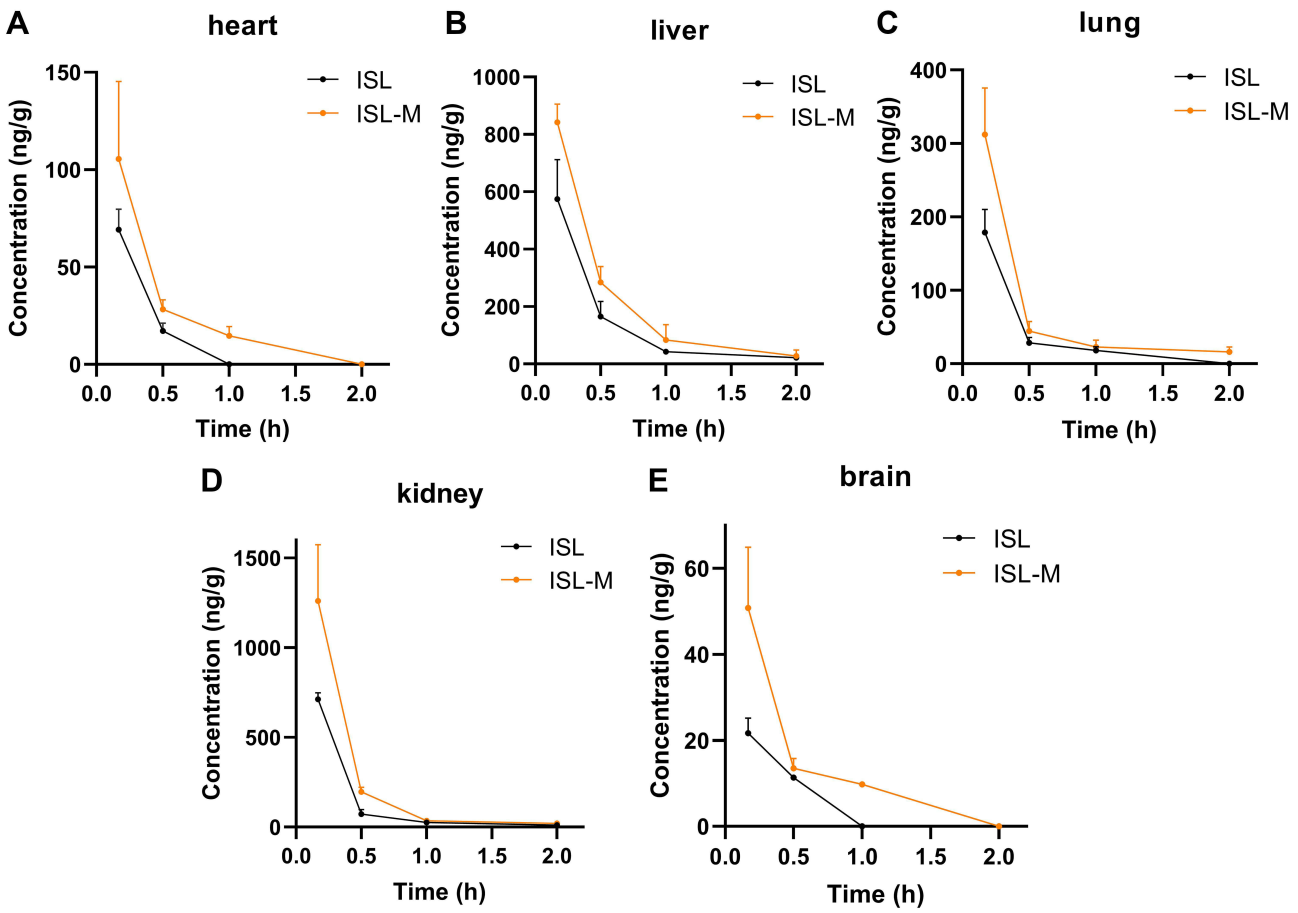

Figure 4 The tissue distribution of ISL in (**A**) heart, (**B**) liver, (**C**) lung, (**D**) kidney and (**E**) brain after single i.v. administration of ISL and ISL-M (2.8 mg/kg) to mice.
Notes: Data was presented as the mean ± SD, n = 4.

Tissue Distribution and Targeting Evaluation of ISL-M

The results in tissue distribution of ISL and ISL-M at different times following an i.v. administration at a dosage of 2.8 mg/kg were shown in Figure 4A–E. The ISL concentration in ISL-M was higher than that of ISL at all time points and in the most of tested tissues. It should be noted that ISL in ISL-M could be measured 1 h after administration, but ISL itself could not be detected at this time in mice. The data in Table 2 illustrated that the values of AUC and C_{max} of ISL from ISL-M were significantly increased compared with that of ISL in all tissues except the heart. In terms of the targeting parameters, the relative rate of uptake (R_e) and the ratio of peak concentration (C_p) of the mouse brain from ISL-M in all

Table 2 Targeting Tissue Evaluation of ISL-M

Tissue	C_{max} (ng/g)		Cp	AUC (ng*h/g)		Re
	ISL	ISL-M		ISL	ISL-M	
Heart	69.15 ± 10.47	105.47 ± 39.84	1.53	18.66 ± 2.11	40.30 ± 7.31**	2.16
Liver	574.44 ± 137.34	841.81 ± 64.01*	1.47	207.70 ± 28.50	335.80 ± 37.09**	1.62
Lung	178.70 ± 31.37	312.03 ± 63.38**	1.75	55.24 ± 6.28	95.79 ± 12.80**	1.73
Kidney	713.19 ± 35.02	1260.57 ± 313.03*	1.77	174.7 ± 9.70	328.5 ± 52.98**	1.88
Brain	21.69 ± 3.45	50.79 ± 14.08**	2.34	8.34 ± 0.61	21.41 ± 2.46***	2.58

Notes: The results were expressed as the mean ± SD, n = 4; vs ISL group: *P < 0.05, **P < 0.01, ***P < 0.001.
Abbreviations: C_{max}, maximum concentration; AUC, area under the concentration–time curve of different tissues; Cp, the ratio of peak concentration; Re, the relative rate of uptake.

tissues were higher than that of ISL, there were significant alteration for the values of R_e and C_p in brain targeted, indicating that ISL-M prepared in our study obviously altered the brain exposure of ISL, increased and prolonged the accumulation in the brain tissue (shown in Figure 4E).

ISL-M Could Decrease Behavioral Impairment in MCAO Mice

The results in Figure 5A showed that there was no significant difference in the longa scores from the MCAO mice in other groups except the sham operation group, indicating that the injury of experimental mice in each group before administration was the same. As shown in Figure 5B, the neurological scores of mice injected with ISL and ISL-M were significantly decreased compared with the MCAO model group. In addition, the weight of mice after MCAO modeling was obviously reduced and the weight recovery rate was also slowed down compared with the sham operation group (see Figure 5C). After treatment with ISL-M, the improvement of perception and motor function in mice was significantly better than that in these mice treated with ISL via the results from the rotarod experiments (see Figure 5D) and the adhesive removal test (shown in Figure 5E and F), suggesting that ISL-M had a more effective protection effect on MCAO brain damage.

Inhibition of Apoptosis and Autophagy of ISL-M in MCAO Mice

It was found that there were some vacuolar in the neurons from the ISL group, and the Nissl bodies were partially disappeared, which was not significantly different from that in the model group (Figure 6A). After ISL-M administration, the dark blue granular Nissl bodies could be clearly seen, and the color was relatively uniform. The number of positive

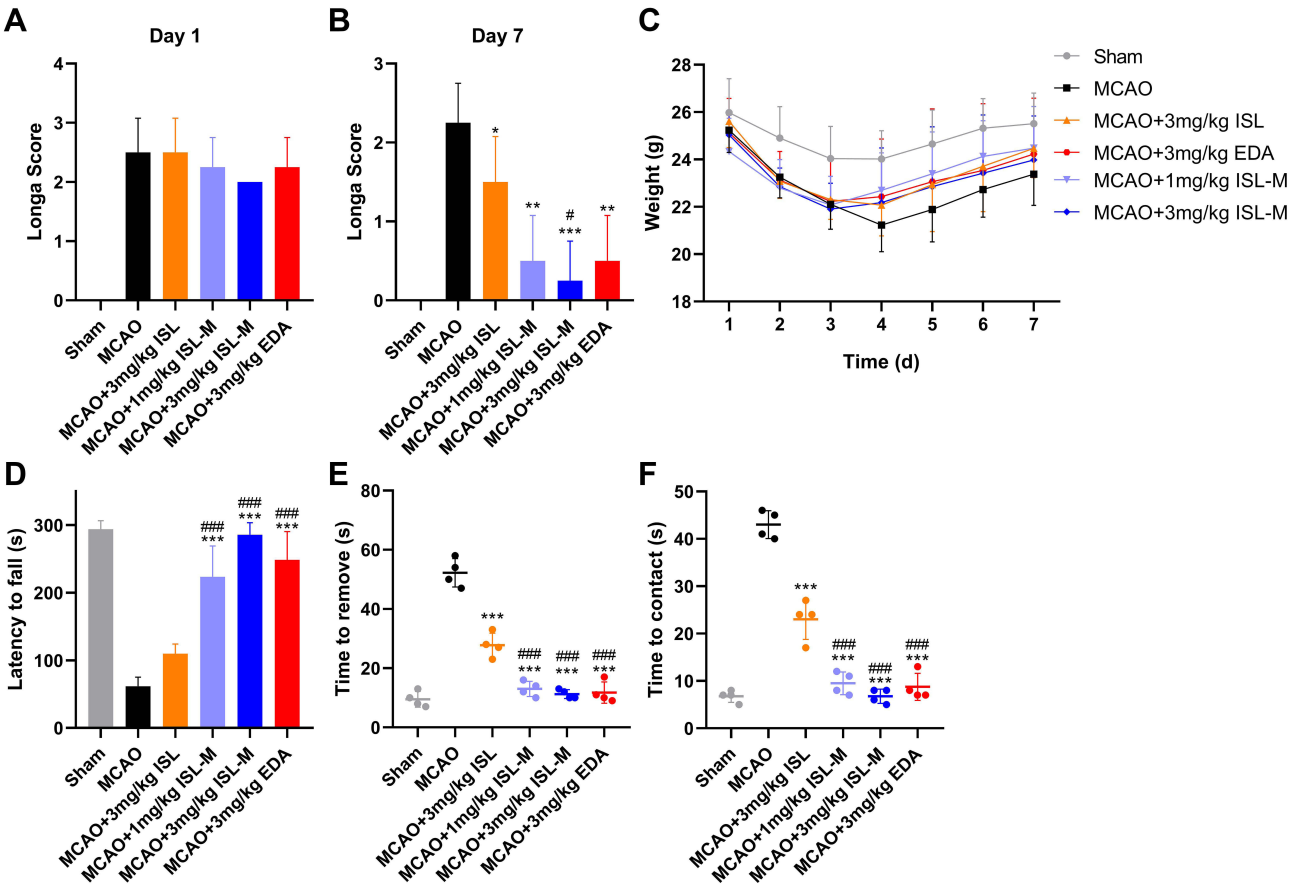

Figure 5 Neuroprotection by the treatment of ISL-M in MCAO-induced ischemic and reperfusion injury. Longa scores of mice in different groups on (**A**) the first and (**B**) seventh days after the operation. (**C**) The weight of mice in different groups in seven days. Behavioral manifestation of MCAO in mice in the rotarod experiments (**D**) and tape removal test (**E** and **F**).

Notes: Data was presented as mean ± SD, n = 4; vs MCAO: *$P < 0.05$, **$P < 0.01$, ***$P < 0.001$; vs MCAO + 3 mg/kg ISL: $^{\#}P < 0.05$, $^{\#\#\#}P < 0.001$.

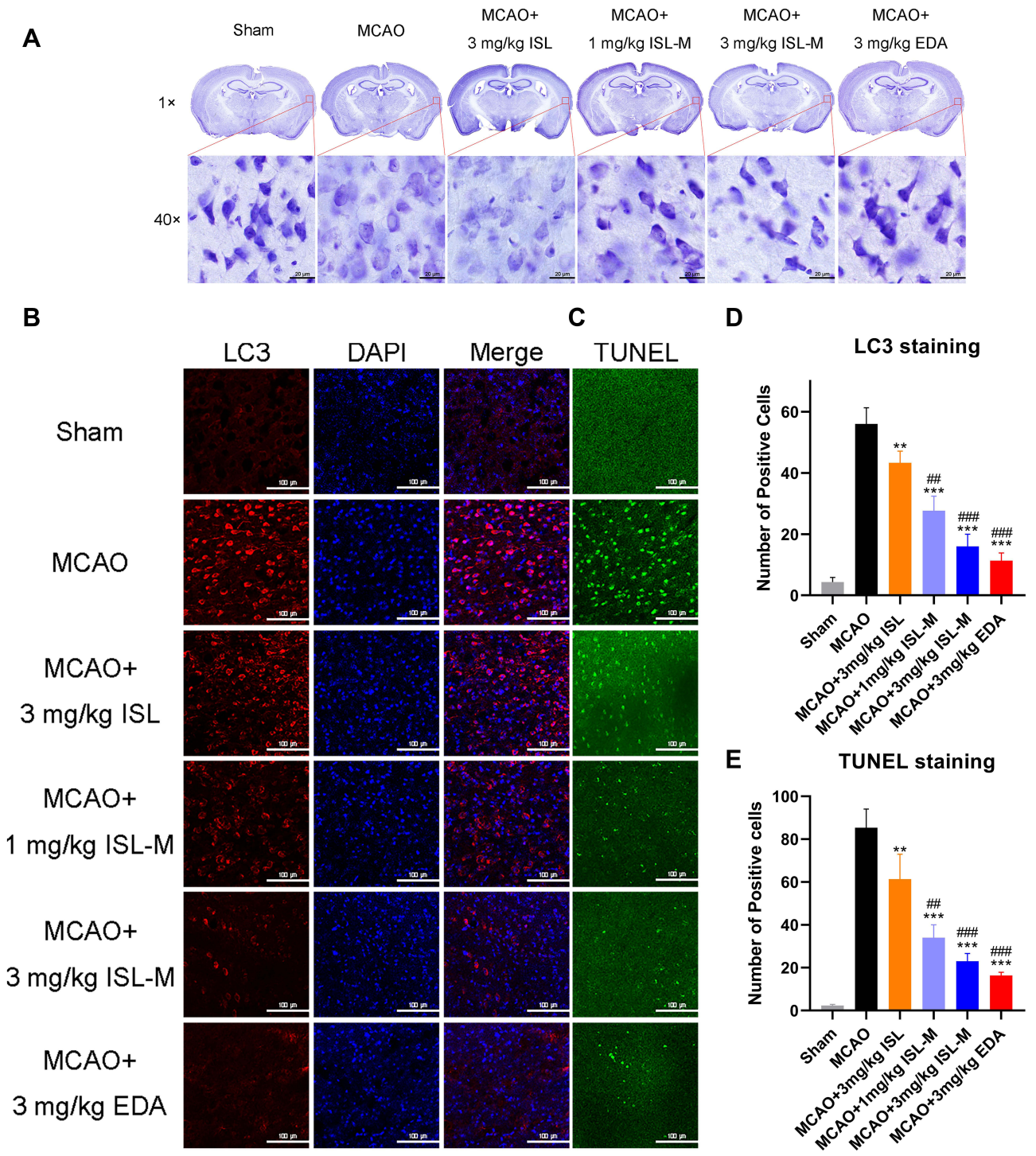

Figure 6 Inhibitory effect on apoptosis and autophagy of ISL-M in MCAO mice model was proved by Nissl staining (**A**) and immunofluorescence staining of LC3 (**B**) and TUNEL (**C**). Record the number of cells in the same fields of view stained with LC3 (**D**) and TUNEL (**E**) by image J.
Notes: Data was presented as mean ± SD, n = 3; vs MCAO: $^{**}P < 0.01$, $^{***}P < 0.001$; vs MCAO + 3 mg/kg ISL: $^{\#\#}P < 0.01$, $^{\#\#\#}P < 0.001$.

cells stained with the TUNEL (Figure 6C and E) and positive cells expressing the LC3 protein (Figure 6B and D) in the ISL group were both less than that in the model group and more than that in the ISL-M group, which showed that ISL-M had a better effect on inhibiting neuronal apoptosis. The presence of LC3 protein was an effective marker for cell autophagy,[41] and the level of autophagy in normal tissue and organism was low. When the homeostasis was destroyed (such as brain injury, ischemia and hypoxia), the autophagy would be induced to remove the excess or damaged

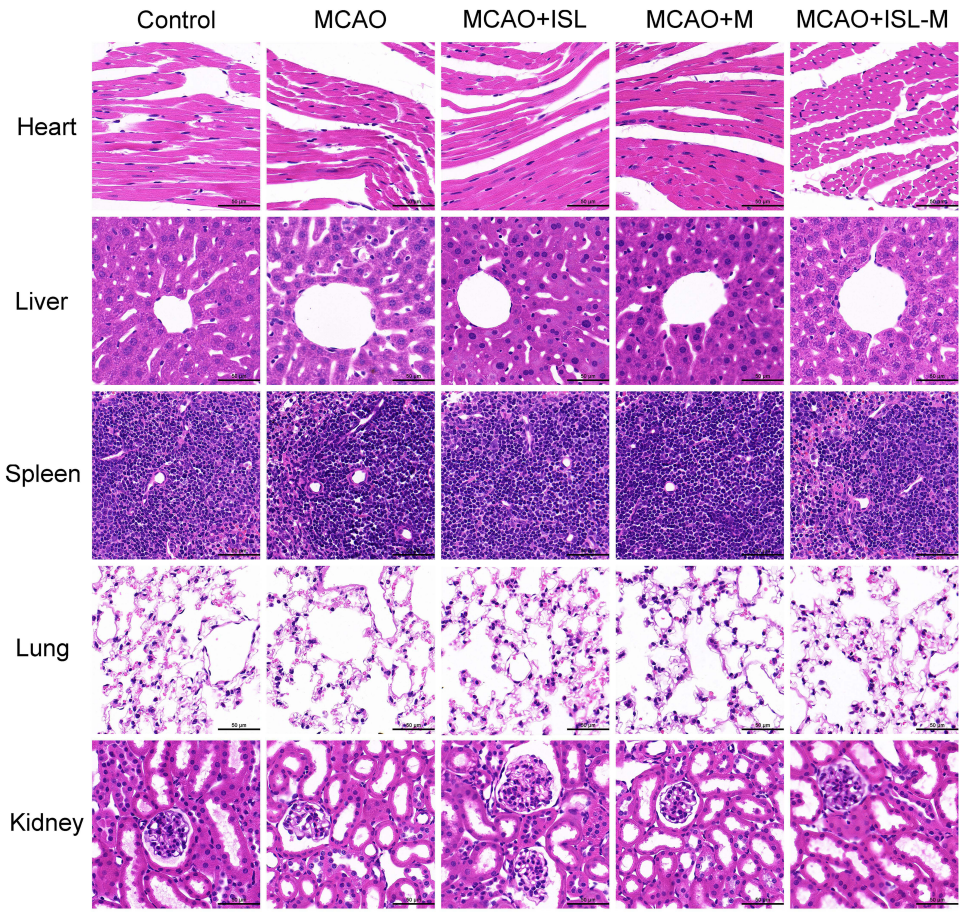

Figure 7 Hematoxylin-eosin staining of heart, liver, spleen, lung and kidney from control, MCAO, MCAO + ISL, MCAO + M, MCAO + ISL-M group of mice (Scale bar: 50 μm).
Abbreviations: MCAO, middle cerebral artery occlusion; M, blank micelles.

organelles and intracellular components.[42–44] Our data indicated that ISL-M could better protect and alleviate the brain injury induced by stroke via inhibition of occurrence or level of autophagy and neuronal apoptosis.

Biocompatibility of Nanoparticles in Major Organs

In order to evaluate the biocompatibility and toxicity of this nanoparticles, the main tissues in mice were paraffin sectioned and stained with the HE in the different tested groups. The results showed that the myocardial cells had the good morphology and complete tissue structures (see Figure 7). In the liver, hepatocytes were also arranged neatly, and the structures of hepatic lobules were not affected by ISL-M. Spleen tissue was also intact, and nanoparticles had no significant effect on the spleen. The structures of lung parenchyma and lung stroma were complete, there was no obvious inflammatory cell infiltration and the lung function was good. We also examined the effect of nanoparticles on the kidney, and found that there were no obviously changes in the structures of glomerulus. In general, the ISL nanoparticles have good biocompatibility in these main tissues and organs.

Conclusions

In this study, we designed a novel ISL loaded nano micelle prepared with DSPE-PEG_{2000} as the drug carrier modified with the brain targeting polypeptide angiopep-2, which have small particle size, good dispersibility, high drug loading and encapsulation efficiency, sustained release effect and pH sensitivity. Compared with the ISL monomers, the ISL nano-micelles could significantly prolong the in vivo circulation time of ISL and enhance the accumulation in the brain tissues via regulating the physicochemical properties of ISL, improving its pharmacokinetic disposition and increasing

brain intake. The ISL-M could ameliorate the brain injury induced by the MCAO mice via inhibition of occurrence or level of cellular autophagy and neuronal apoptosis. There were no cellular structural damages and other adverse effects for ISL-M on the main tissues and organs. Our data further confirmed that the ISL-M could improve the ischemic stroke effect. In conclusion, our ISL-M could serve as a promising, ideal and effective candidate for the clinical application of ISL in the treatment of acute ischemic stroke.

Acknowledgments

This study was supported by the National Foundation of Natural Sciences of China (Grant No. 82073925 and 81773803).

Disclosure

The authors have no conflicts of interest to declare.

References

1. Feigin VL, Nichols E, Alam T.; G.B.D.N. Collaborators. Global, regional, and national burden of neurological disorders, 1990–2016: a systematic analysis for the global burden of disease study 2016. *Lancet Neurol*. 2019;18:459–480. doi:10.1016/S1474-4422(18)30499-X
2. Virani SS, Alonso A, Benjamin EJ, et al. Heart disease and stroke statistics-2020 update: a report from the American Heart Association. *Circulation*. 2020;141:139–596.
3. Powers WJ, Rabinstein AA, Ackerson T, et al. 2018 guidelines for the early management of patients with acute ischemic stroke: a guideline for healthcare professionals from the American Heart Association/American Stroke Association. *Stroke*. 2018;49:46–110. doi:10.1161/STR.0000000000000158
4. Yu H, Li H, Li Y, Li M, Chen G. Effect of isoliquiritigenin for the treatment of atopic dermatitis-like skin lesions in mice. *Arch Dermatol Res*. 2017;309:805–813. doi:10.1007/s00403-017-1787-3
5. Vaya J, Belinky PA, Aviram M. Antioxidant constituents from licorice roots: isolation, structure elucidation and antioxidative capacity toward LDL oxidation. *Free Radic Biol Med*. 1997;23:302–313. doi:10.1016/S0891-5849(97)00089-0
6. Ning S, Ma X, Zhu D, et al. Isoliquiritigenin attenuates MiR-21 expression via induction of PIAS3 in breast cancer cells. *Rsc Adv*. 2017;7:18085–18092. doi:10.1039/C6RA25511F
7. Zhan C, Yang J. Protective effects of isoliquiritigenin in transient middle cerebral artery occlusion-induced focal cerebral ischemia in rats. *Pharmacol Res*. 2006;53:303–309. doi:10.1016/j.phrs.2005.12.008
8. Lukyanov AN, Torchilin VP. Micelles from lipid derivatives of water-soluble polymers as delivery systems for poorly soluble drugs. *Adv Drug Deliv Rev*. 2004;56:1273–1289. doi:10.1016/j.addr.2003.12.004
9. Torchilin VP. Micellar nanocarriers: pharmaceutical perspectives. *Pharm Res*. 2007;24:1–16. doi:10.1007/s11095-006-9132-0
10. Li X, Hou X, Ding W, et al. Sirolimus-loaded polymeric micelles with honokiol for oral delivery. *J Pharm Pharmacol*. 2015;67:1663–1672. doi:10.1111/jphp.12482
11. Gill KK, Nazzal S, Kaddoumi A. Paclitaxel loaded PEG (5000)-DSPE micelles as pulmonary delivery platform: formulation characterization, tissue distribution, plasma pharmacokinetics, and toxicological evaluation. *Eur J Pharm Biopharm*. 2011;79:276–284. doi:10.1016/j.ejpb.2011.04.017
12. Krishnadas A, Rubinstein I, Onyüksel H. Sterically stabilized phospholipid mixed micelles: in vitro evaluation as a novel carrier for water-insoluble drugs. *Pharm Res*. 2003;20:297–302. doi:10.1023/A:1022243709003
13. Onyüksel H, Ikezaki H, Patel M, Gao XP, Rubinstein I. A novel formulation of VIP in sterically stabilized micelles amplifies vasodilation in vivo. *Pharm Res*. 1999;16:155–160. doi:10.1023/A:1018847501985
14. Alexis F, Pridgen E, Molnar LK, Farokhzad OC. Factors affecting the clearance and biodistribution of polymeric nanoparticles. *Mol Pharm*. 2008;5:505–515. doi:10.1021/mp800051m
15. De Oliveira Junior ER, Santos LCR, Salomao MA, et al. Nose-to-brain drug delivery mediated by polymeric nanoparticles: influence of PEG surface coating. *Drug Deliv Transl Res*. 2020;10:1688–1699. doi:10.1007/s13346-020-00816-2
16. Pardridge WM. Blood-brain barrier drug targeting: the future of brain drug development. *Mol Interv*. 2003;3:90–105. doi:10.1124/mi.3.2.90
17. Pardridge WM. Blood-brain barrier delivery. *Drug Discov Today*. 2007;12:54–61. doi:10.1016/j.drudis.2006.10.013
18. Löscher W, Potschka H. Drug resistance in brain diseases and the role of drug efflux transporters. *Nat Rev Neurosci*. 2005;6:591–602. doi:10.1038/nrn1728
19. Demeule M, Régina A, Ché C, Poirier J, Béliveau R. Identification and design of peptides as a new drug delivery system for the brain. *J Pharmacol Exp Ther*. 2008;324:1064–1072. doi:10.1124/jpet.107.131318
20. Rip J, Schenk GJ, de Boer AG. Differential receptor-mediated drug targeting to the diseased brain. *Expert Opin Drug Deliv*. 2009;6:227–237. doi:10.1517/17425240902806383
21. Jones AR, Shusta EV. Blood-brain barrier transport of therapeutics via receptor-mediation. *Pharm Res*. 2007;24:1759–1771. doi:10.1007/s11095-007-9379-0
22. Bhandari R, Kaur IP. Pharmacokinetics, tissue distribution and relative bioavailability of isoniazid-solid lipid nanoparticles. *Int J Pharm*. 2013;441:202–212. doi:10.1016/j.ijpharm.2012.11.042
23. Hao HP, Wang G, Cui N, et al. Pharmacokinetics, absorption and tissue distribution of tanshinone IIA solid dispersion. *Planta Med*. 2006;72:1311–1317. doi:10.1055/s-2006-951698
24. Longa EZ, Weinstein PR, Carlson S, Cummins R. Reversible middle cerebral artery occlusion without craniectomy in rats. *Stroke*. 1989;20:84–91. doi:10.1161/01.STR.20.1.84
25. Liu ZJ, Ran Y, Huang S, et al. Curcumin protects against ischemic stroke by titrating microglia/macrophage polarization. *Front Aging Neurosci*. 2017;9:233. doi:10.3389/fnagi.2017.00233

26. Zausinger S, Hungerhuber E, Baethmann A, Reulen H, Schmin-Elsaesser R. Neurological impairment in rats after transient middle cerebral artery occlusion: a comparative study under various treatment paradigms. *Brain Res*. 2000;863:94–105. doi:10.1016/S0006-8993(00)02100-4
27. Yan HM, Wei P, Song J, Jia X, Zhang Z. Enhanced anticancer activity in vitro and in vivo of luteolin incorporated into long-circulating micelles based on DSPE-PEG2000 and TPGS. *J Pharm Pharmacol*. 2016;68:1290–1298. doi:10.1111/jphp.12598
28. Dreaden EC, Austin LA, Mackey MA, EI-Sayed MA. Size matters: gold nanoparticles in targeted cancer drug delivery. *Ther Deliv*. 2012;3:457–478. doi:10.4155/tde.12.21
29. Zuckerman JE, Choi CHJ, Han H, Davis ME. Polycation-siRNA nanoparticles can disassemble at the kidney glomerular basement membrane. *Proc Natl Acad Sci USA*. 2012;109:3137–3142. doi:10.1073/pnas.1200718109
30. De Barros AB, Tsourkas A, Saboury B, Cardoso VN, Alavi A. Emerging role of radiolabeled nanoparticles as an effective diagnostic technique. *EJNMMI Res*. 2012;2:39. doi:10.1186/2191-219X-2-39
31. Kulkarni SA, Feng SS. Effects of particle size and surface modification on cellular uptake and biodistribution of polymeric nanoparticles for drug delivery. *Pharmaceut Res*. 2013;30:2512–2522. doi:10.1007/s11095-012-0958-3
32. Faraji AH, Wipf P. Nanoparticles in cellular drug delivery. *Bioorg Med Chem*. 2009;17:2950–2962. doi:10.1016/j.bmc.2009.02.043
33. Liu X, Huang N, Li H, Jin Q, Ji J. Surface and size effects on cell interaction of gold nanoparticles with both phagocytic and nonphagocytic cells. *Langmuir*. 2013;29:9138–9148. doi:10.1021/la401556k
34. Huang J, Bu L, Xie J, et al. Effects of nanoparticle size on cellular uptake and liver MRI with polyvinylpyrrolidone-coated iron oxide nanoparticles. *ACS Nano*. 2010;4:7151–7160. doi:10.1021/nn101643u
35. Lu F, Wu SH, Hung Y, Mou CY. Size effect on cell uptake in well-suspended, uniform mesoporous silica nanoparticles. *Small*. 2009;5:1408–1413. doi:10.1002/smll.200900005
36. Wang SH, Lee CW, Chiou A, Wei PK. Size-dependent endocytosis of gold nanoparticles studied by three-dimensional mapping of plasmonic scattering images. *J Nanobiotechnol*. 2010;8:33. doi:10.1186/1477-3155-8-33
37. Cruje C, Chithrani BD. Integration of peptides for enhanced uptake of PEGylayed gold nanoparticles. *J Nanosci Nanotechnol*. 2015;15:2125–2131. doi:10.1166/jnn.2015.10321
38. Jindal AB. The effect of particle shape on cellular interaction and drug delivery applications of micro- and nanoparticles. *Int J Pharm*. 2017;532:450–465. doi:10.1016/j.ijpharm.2017.09.028
39. Laouini A, Jaafar-Maalej C, Limayem-Blouza I, et al. Preparation, characterization and applications of liposomes: state of the art. *J Colloid Sci Biotechnol*. 2012;1:147–168. doi:10.1166/jcsb.2012.1020
40. Croy SR, Kwon GS. Polymeric micelles for drug delivery. *Curr Pharm Des*. 2006;12:4669–4684. doi:10.2174/138161206779026245
41. Kabeya Y, Mizushima N, Yamamoto A, et al. LC3, GABARAP and GATE16 localize to autophagosomal membrane depending on form-II formation. *J Cell Sci*. 2004;117:2805–2812. doi:10.1242/jcs.01131
42. Yoshimori T. Autophagy: a regulated bulk degradation process inside cells. *Biochem Biophys Res Commun*. 2004;313:453–458. doi:10.1016/j.bbrc.2003.07.023
43. Reggiori F, Klionsky DJ. Autophagosomes: biogenesis from scratch. *Curr Opin Cell Biol*. 2005;17:415–422. doi:10.1016/j.ceb.2005.06.007
44. Kurz T, Terman A, Brunk UT. Autophagy, ageing and apoptosis: the role of oxidative stress and lysosomal iron. *Arch Biochem Biophys*. 2007;462:220–230. doi:10.1016/j.abb.2007.01.013